

Anomalous Hall effect in three ferromagnetic compounds: $\text{EuFe}_4\text{Sb}_{12}$, $\text{Yb}_{14}\text{MnSb}_{11}$, and $\text{Eu}_8\text{Ga}_{16}\text{Ge}_{30}$

Brian C. Sales, Rongying Jin, and David Mandrus

Materials Science and Technology Division, Oak Ridge National Laboratory, Oak Ridge, Tennessee 37831, USA

Peter Khalifah

Materials Science and Technology Division, Oak Ridge National Laboratory, Oak Ridge, Tennessee 37831, USA and Department of Chemistry, University of Massachusetts, Amherst, Massachusetts 01003, USA

(Received 1 March 2006; revised manuscript received 9 May 2006; published 27 June 2006)

The Hall resistivity (ρ_{xy}), resistivity (ρ_{xx}), and magnetization of three metallic ferromagnets are investigated as a function of magnetic field and temperature. The three ferromagnets, $\text{EuFe}_4\text{Sb}_{12}$ ($T_c \approx 84$ K), $\text{Yb}_{14}\text{MnSb}_{11}$ ($T_c \approx 53$ K), and $\text{Eu}_8\text{Ga}_{16}\text{Ge}_{30}$ ($T_c \approx 36$ K) are Zintl compounds with carrier concentrations between 1×10^{21} and 3.5×10^{21} cm^{-3} . The relative decrease in ρ_{xx} below T_c [$\rho_{xx}(T_c)/\rho_{xx}(2\text{ K})$] is 28, 6.5, and 1.3 for $\text{EuFe}_4\text{Sb}_{12}$, $\text{Yb}_{14}\text{MnSb}_{11}$, and $\text{Eu}_8\text{Ga}_{16}\text{Ge}_{30}$, respectively. The low carrier concentrations coupled with low magnetic anisotropies allow a relatively clean separation between the anomalous (ρ'_{xy}), and normal contributions to the measured Hall resistivity. For each compound the anomalous contribution in the zero field limit is fit to $a\rho_{xx} + \sigma_{xy}\rho_{xx}^2$ for temperatures $T < T_c$. At $T=0$ the anomalous Hall conductivity σ'_{xy} , is -220 ± 5 ($\Omega^{-1}\text{cm}^{-1}$), -14.7 ± 1 ($\Omega^{-1}\text{cm}^{-1}$), and 28 ± 3 ($\Omega^{-1}\text{cm}^{-1}$) for $\text{EuFe}_4\text{Sb}_{12}$, $\text{Yb}_{14}\text{MnSb}_{11}$, and $\text{Eu}_8\text{Ga}_{16}\text{Ge}_{30}$, respectively, and is independent of temperature for $T < T_c$ if the change in spontaneous magnetization (order parameter) with temperature is taken into account. These data are consistent with recent theories [T. Jungwirth, Q. Niu, and A. H. MacDonald, *Phys. Rev. Lett.* **88**, 207208 (2002); Y. Yao, L. Kleinman, A. H. MacDonald, J. Sinova, T. Jungwirth, D.-S. Wang, E. Wang, and Q. Niu, *Phys. Rev. Lett.* **92**, 037204 (2004); I. V. Solov'yev, *Phys. Rev. B* **67**, 174406 (2003); Z. Fang, N. Nagaosa, K. S. Takahashi, A. Asamitsu, R. Mathieu, T. Ogasawara, H. Yamada, M. Kawasaki, Y. Tokura, and K. Terakura, *Science* **302**, 92 (2003); and Y. Taguchi, Y. Oohara, H. Yoshizawa, N. Nagaosa, and Y. Tokura, *Science* **291**, 2573 (2001)] of the anomalous Hall effect that suggest that even for stoichiometric ferromagnetic crystals, such as those studied in this article, the intrinsic Hall conductivity is finite at $T=0$, and is a ground state property that can be calculated from the electronic structure.

DOI: 10.1103/PhysRevB.73.224435

PACS number(s): 75.47.-m, 75.50.Cc

INTRODUCTION

The origin of the large “anomalous” contribution to the Hall resistivity of ferromagnets has remained a source of confusion since the seminal experiments of Hall^{1,2} in the 1880s. The quantity measured in a standard dc Hall experiment is the Hall resistivity $\rho_{xy} = E_y/J_x = V_y d/I_x$ where a dc current I_x flows through a rectangular slab of thickness d in the x direction, the voltage is measured across the sample in the y direction with a magnetic field B applied along the z direction. In materials with no significant magnetism, the Hall resistivity is proportional to the applied magnetic field and describes the effect of the Lorentz force on the motion of the free carriers. In simple one band materials the Hall resistivity can be used to measure the type (electrons or holes) and number of carriers. In ferromagnetic compounds or materials with a substantial magnetic susceptibility, there is an additional contribution to the Hall resistivity that is proportional to the magnetization, M , of the material and is usually at least one order of magnitude larger than the Lorentz term. For a magnetic material the Hall resistivity is described by $\rho_{xy} = R_o B + R_s 4\pi M = R_o B + \rho'_{xy}$ where $R_o B$ is the ordinary contribution and ρ'_{xy} describes the anomalous contribution to the Hall effect (AHE). In a good metal (like iron) the coefficient R_s is much larger than R_o . Various theories³⁻⁶ of the origin R_s have shown that R_s can be described by intrinsic and extrinsic contributions that are proportional to ρ^2 or ρ , respectively,

where ρ is the zero field resistivity $\rho = \rho_{xx}(0)$. The extrinsic contribution^{3,4} accounts for the skew scattering of carriers by magnetic impurities and defects but is hard to quantitatively model in real materials. The pioneering work of Karplus and Luttinger,⁶ however, showed there was an intrinsic contribution to the AHE that arose from the spin-orbit coupling of Bloch bands, i.e., a contribution that in principle could be extracted from the calculated electronic structure. Thus the anomalous Hall resistivity *in zero applied magnetic field*, ρ'_{xy} can be parametrized⁷ by $\rho'_{xy} = \sigma'_{xy}\rho^2 + a\rho$, where σ'_{xy} is the intrinsic anomalous Hall conductivity, and a describes the extrinsic contribution of skew scattering. We emphasize that in zero applied field the normal Hall contribution is zero and the anomalous contribution vanishes when $T > T_c$. To be consistent with the notation used in the theoretical calculations we set $\sigma'_{xy} = \sigma_{xy}$. In the case of Fe metal, the calculations of Yao *et al.*⁸ predict an intrinsic Hall conductivity of $\sigma_{xy} = 751$ ($\Omega\text{cm})^{-1}$ at $T=0$ and $\sigma_{xy} = 734$ ($\Omega\text{cm})^{-1}$ at $T=300$ K as compared to the room temperature experimental⁹ value of 1032 ($\Omega\text{cm})^{-1}$. An interesting consequence of this calculation is that temperature has very little effect on σ_{xy} as long as there is no significant change in the magnetization over the temperature range of interest. This observation has important consequences on the best way to separate the intrinsic and extrinsic contributions from experimental data.^{7,10}

In the present article, we investigate the intrinsic and extrinsic contributions to the AHE in three unusual ferromag-

nets: $\text{EuFe}_4\text{Sb}_{12}$, $\text{Yb}_{14}\text{MnSb}_{11}$, and $\text{Eu}_8\text{Ga}_{16}\text{Ge}_{30}$. All three ferromagnets are stoichiometric Zintl compounds^{11,12} which implies both ionic and covalent bonds. The compounds can be regarded as heavily doped semiconductors or bad metals with typical carrier concentrations of $1\text{--}3.5 \times 10^{21}$ carriers/cm³. The dominant carriers are holes in $\text{EuFe}_4\text{Sb}_{12}$ and $\text{Yb}_{14}\text{MnSb}_{11}$ and electrons in $\text{Eu}_8\text{Ga}_{16}\text{Ge}_{30}$. Although the three compounds are magnetically soft ferromagnets, the crystal structures are relatively complex with 34, 208, and 54 atoms in the conventional unit cell, respectively. One of the goals of the present work is to see how well current thinking about the origin of the AHE applies to more complex materials.

SYNTHESIS AND EXPERIMENTAL METHODS

The synthesis of $\text{EuFe}_4\text{Sb}_{12}$, $\text{Yb}_{14}\text{MnSb}_{11}$ and $\text{Eu}_8\text{Ga}_{16}\text{Ge}_{30}$ has been described in detail previously.^{13–16} Briefly, $\text{EuFe}_4\text{Sb}_{12}$ was prepared directly from the elements in a carbon-coated, evacuated and sealed silica tube. The tube was heated to 1030 °C for 40 h, quenched into a water bath, and then heated at 700 °C for one week to form the correct cubic skutterudite phase. The resulting powder was ball milled in Ar gas, and then hot pressed in vacuum in a graphite die into a dense polycrystalline solid. The density of the hot-pressed polycrystalline sample was 98% of the theoretical x-ray density of 7.98 g/cm³. X-ray diffraction confirmed that the samples were single phase with the cubic skutterudite structure (space group $Im\bar{3}$, lattice constant $a = 0.917$ nm, 34 atoms per unit cell). From x-ray structure refinements the estimated filling of the Eu site was 0.95, a value comparable to that found in single crystals.¹⁷ Heat capacity, magnetization, and resistivity measurements on the hot pressed sample indicate $\text{EuFe}_4\text{Sb}_{12}$ becomes ferromagnetic below about 84 K, a value similar to that reported by Bauer¹⁸ but a little lower than the value of 87 K reported for a single crystal.¹⁷ A thinned polycrystalline plate is used for the Hall and resistivity measurements.

Crystals of $\text{Yb}_{14}\text{MnSb}_{11}$ were grown from a Sn flux using the method described by Fisher *et al.*¹⁴ This phase, originally reported by Chan *et al.*,¹⁹ crystallizes with a tetragonal lattice in the space group $I41/acd$ with $a = 1.661$ nm and $c = 2.195$ nm, and 208 atoms in the conventional unit cell. Heat capacity, resistivity, and magnetization data on $\text{Yb}_{14}\text{MnSb}_{11}$ crystals indicate ferromagnetism below 53 K.^{14,15} A thinned single crystal plate with $H \parallel (110)$ and current along c is used for the Hall measurements.

The cubic clathrate compound $\text{Eu}_8\text{Ga}_{16}\text{Ge}_{30}$ (space group $Pm\bar{3}n$, $a = 1.070$ nm, 54 atoms in unit cell) could be prepared by several methods, the simplest of which was the direct arc melting together of the elements on a water-cooled copper hearth in an Ar atmosphere. Crystals are also grown by cooling a stoichiometric melt of the elements in a carbon coated silica ampoule.¹⁶ A small unoriented single crystal plate [$H \approx \parallel(4\ 3\ 2)$] of $\text{Eu}_8\text{Ga}_{16}\text{Ge}_{30}$ is used in the present experiments with $T_c \approx 36$ K. The crystal was not large enough to orient it along a principle direction, but we note that since the crystal structure is cubic, the resistivity is isotropic, and the Hall resistivity is not likely to show much variation with orientation.

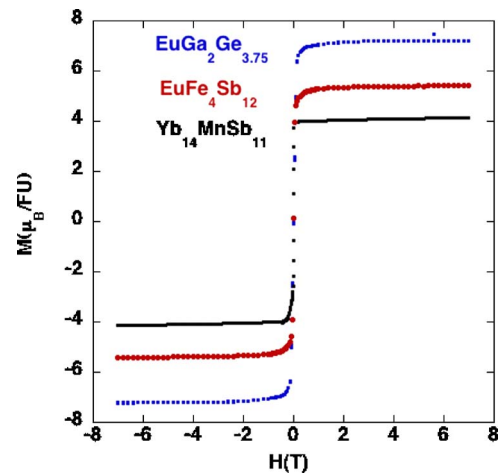


FIG. 1. (Color online) Magnetization vs magnetic field at 5 K for the three ferromagnetic compounds.

Hall effect, resistivity, and heat capacity data are taken using a physical property measurement system from Quantum Design. Hall and resistivity data are obtained using a standard six lead method and either rotating the sample by 180° in a fixed magnetic field or by sweeping the direction of the field from positive to negative values. Low resistance electrical contacts are made to $\text{EuFe}_4\text{Sb}_{12}$ with silver epoxy, and to $\text{Yb}_{14}\text{MnSb}_{11}$ with silver paste. For the $\text{Eu}_8\text{Ga}_{16}\text{Ge}_{30}$ crystals, however, the surface is first etched with Ar ions and then sputter coated with gold pads. Silver paste is used to attach 0.025-mm-diam Pt wires to the gold pads. The Hall data from the three materials are qualitatively the same regardless of the orientation of the crystal with respect to the current or field directions. Magnetization data are taken using a commercial superconducting quantum interference device magnetometer from Quantum Design.

MAGNETIC DATA AND BACKGROUND INFORMATION

Magnetization curves at 5 K for the three compounds are shown in Fig. 1. For each ferromagnet there is very little hysteresis and the full saturation moment is reached at relatively low applied magnetic fields ($H < 1$ T). The magnetic anisotropy is small (a few hundred Gauss) for the cubic compounds ($\text{EuFe}_4\text{Sb}_{12}$ and $\text{Eu}_8\text{Ga}_{16}\text{Ge}_{30}$) while for $\text{Yb}_{14}\text{MnSb}_{11}$ the maximum anisotropy corresponds to a field of about 1 T [i.e., if the field is applied along the magnetically hard (110) direction it takes about 1 T to reach full saturation at 2 K]. The magnetization data for $\text{Yb}_{14}\text{MnSb}_{11}$ shown in Fig. 1 is taken with the applied field along the easy (001) direction.

The magnetization curve for $\text{Eu}_8\text{Ga}_{16}\text{Ge}_{30}$ is the simplest to understand since the saturation magnetization nearly corresponds to the ionic Hund's rule value of $7 \mu_B$ per Eu^{2+} . The large separation distance between neighboring Eu^{2+} ions in the $\text{Eu}_8\text{Ga}_{16}\text{Ge}_{30}$ structure (about 5.4 Å), and the poor bonding between the Eu^{2+} ions and the Ga and Ge atoms forming a cage around each Eu suggests that the magnetic order in this material occurs via a Ruderman-Kittel-(Kasuya)-Yoshida (RK(K)Y) indirect exchange interaction.^{16,20,21} There are two types of Ge-Ga cages in the

type-I clathrate structure corresponding to polyhedra consisting of either 20 (small cage) or 24 (large cage) atoms of Ge or Ga with Eu ions residing near the center of each cage. In the large cage, the Eu is poorly bonded and moves off center to one of four nearly equivalent sites.¹⁶

Remarkably, Mossbauer and rf absorption measurements show that the Eu ions actually tunnel among the four sites at a slow frequency of about 450 MHz!²² Elastic constant measurements and theory also suggest (although indirectly) a similar tunneling frequency.²³ The slow dynamics due to movement of the Eu ions in the large cages does not appear to affect the dc magnetic properties, but may contribute to the unusually low carrier mobility well below T_c .

The compound $\text{Yb}_{14}\text{MnSb}_{11}$ may be a rare example of an under-screened Kondo lattice.^{15,24} In the material all of the Yb ions are divalent and hence nonmagnetic. The magnetism comes from the Mn 3d electrons and the antiferromagnetic coupling of these electrons to holes in the Sb 5p bands. The shortest Mn-Mn distance in $\text{Yb}_{14}\text{MnSb}_{11}$ is 1.0 nm. The electronic state of the Mn is believed to be the d^5 +hole configuration that is found, for example, in GaAs doped with Mn.²⁵ The antiferromagnetic coupling between a local magnetic moment and extended Bloch states can result in ferromagnetism due to the RK(K)Y interaction, but can also give rise to Kondo physics. In $\text{Yb}_{14}\text{MnSb}_{11}$, the ferromagnetic ground state is accompanied by a substantial ($\approx 20 m_e$) mass enhancement of the holes near the Fermi energy. A reduction of the hole concentration in $\text{Yb}_{14}\text{MnSb}_{11}$ by chemical replacement of 5% of the Yb by La, lowers T_c to 39 K, but increases the ferromagnetic saturation moment because there are fewer carriers to screen the Mn d^5 moment.¹⁵

The ferromagnetism of the filled skutterudite $\text{EuFe}_4\text{Sb}_{12}$ is more complex than we initially thought. The skutterudite compounds with divalent cations, such as $\text{CaFe}_4\text{Sb}_{12}$, are incipient band ferromagnets^{26,27} in the sense of the Stoner model. A further increase in the carrier concentration by the replacement of divalent Ca by monovalent Na, results in a ferromagnet²⁸ with a T_c of 85 K, surprisingly close to the 84 K of $\text{EuFe}_4\text{Sb}_{12}$. This suggests that the polarization of the Fe 3d bands caused by the substitution of Ca by magnetic Eu ions is enough to drive the compound ferromagnetic. In addition, careful Mossbauer²² and x-ray magnetic circular dichromism measurements²⁹ on our $\text{Eu}_{0.95}\text{Fe}_4\text{Sb}_{12}$ samples indicate that about 10%–15% of the Eu is Eu^{3+} , which has a nonmagnetic $J=0$ ground state. The dichromism measurements also show a small moment of ≈ 0.1 – $0.2 \mu_B$ per Fe, and that this moment is oriented opposite to the Eu^{2+} moment. Taken together, all of these effects predict a saturation moment of about $5 \mu_B$ per formula unit of $\text{EuFe}_4\text{Sb}_{12}$, which is near the value measured in Fig 1.

As discussed in the Introduction, the Hall resistivity of a ferromagnet is described by $\rho_{xy} = R_o B + R_s 4\pi M$, where the second term is the anomalous contribution to the Hall resistivity. If a relatively small magnetic field is applied ($H < 1$ T) to a soft ferromagnet, essentially all of the domains will be aligned and the Hall resistivity will be dominated by the second term. As the temperature is increased to an appreciable fraction of T_c , however, the maximum value of M will depend on how the spontaneous magnetization (order parameter) changes with temperature. This behavior is illustrated

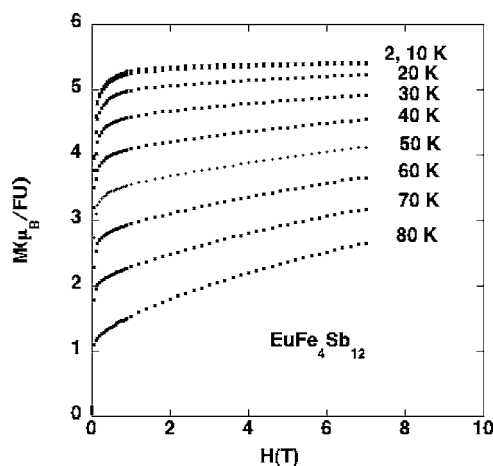


FIG. 2. Magnetization vs magnetic field at various temperatures for the ferromagnet $\text{EuFe}_4\text{Sb}_{12}$.

by the magnetization curves shown in Fig. 2 for $\text{EuFe}_4\text{Sb}_{12}$. For temperatures not too close to T_c ($T < 0.9 T_c$) the approximate variation of the order parameter with T can be estimated by extrapolating the high field portion of the magnetization curves back to $H=0$. Alternately, the magnetization versus temperature can be measured at the lowest field ($H \approx 1$ T) where all of the domains are aligned. Both analyses give essentially the same variation of $M(T)/M(0)$ with T/T_c as shown in Fig. 3.

RESISTIVITY AND HALL DATA

The dc resistivity versus temperature for each ferromagnet is shown in Fig. 4(a). At room temperature the magnitude of the resistivity is similar for all three compounds with values of 0.38, 0.54, and $1.7 \text{ m}\Omega \text{ cm}$ for $\text{EuFe}_4\text{Sb}_{12}$, $\text{Eu}_8\text{Ga}_{16}\text{Ge}_{30}$, and $\text{Yb}_{14}\text{MnSb}_{11}$, respectively. The resistivity

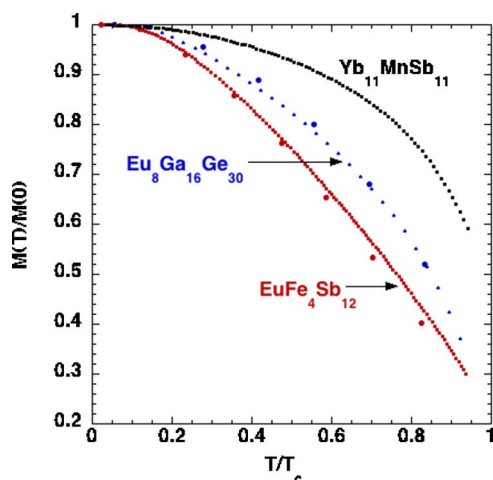


FIG. 3. (Color online) Normalized magnetization $M(T)/M(0)$ vs T/T_c for the three ferromagnets. The larger points correspond to estimates of $M(T)/M(0)$ obtained from magnetization curves such as shown in Fig. 2. The remaining data were obtained from magnetization vs temperature measurements with an applied field of 1 T. $M(0)$ is the value of the magnetization at 2 K.

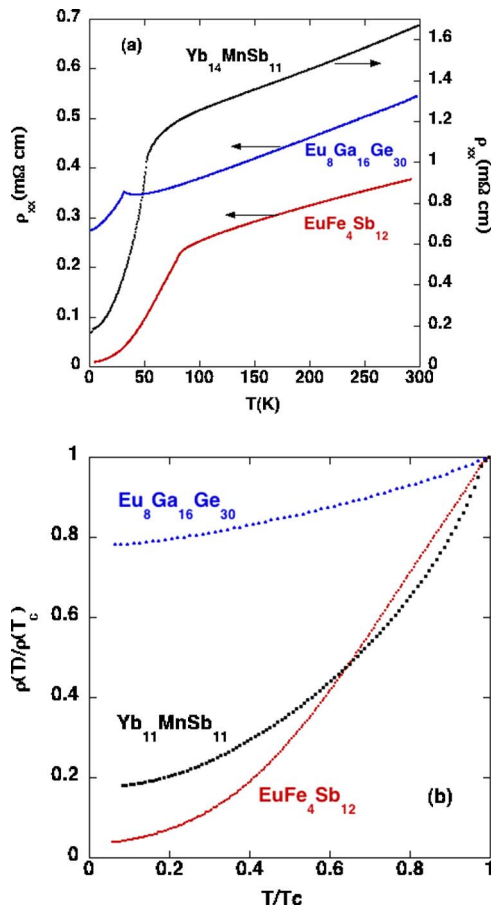


FIG. 4. (Color online) (a) Resistivity vs temperature for the three ferromagnets. The data for the Yb₁₄MnSb₁₁ crystal is taken with the current along the c axis. (b) Normalized resistivity vs T/T_c for the three ferromagnets.

of tetragonal Yb₁₄MnSb₁₁ is measured with the current along the (001) direction. These values are suggestive of a heavily doped semiconductor or a bad metal. Below the ferromagnetic transition temperature of each compound there is a rapid decrease in the resistivity due to the loss of spin disorder scattering. The relative decrease in the resistivity below T_c is defined as $[\rho(T_c)/\rho(2\text{ K})]$ and is 28, 6.5, and 1.3 for EuFe₄Sb₁₂, Yb₁₄MnSb₁₁, and Eu₈Ga₁₆Ge₃₀, respectively. The relatively small change in the resistivity with temperature for the Eu₈Ga₁₆Ge₃₀ single crystal is probably due to the random distribution of Ga and Ge on the framework sites and the disorder due to the Eu atoms in the larger cages slowly tunneling or hopping among four off center positions. The normalized resistivity for each compound below T_c is shown in Fig. 4(b). These data illustrate the relatively large decrease in the resistivity of EuFe₄Sb₁₂ and Yb₁₄MnSb₁₁ below T_c , which makes possible an accurate evaluation of the dependence of the AHE on ρ and ρ^2 .

The Hall resistivity at 7 T versus temperature is shown in Fig. 5 for all three compounds. For EuFe₄Sb₁₂ and Eu₈Ga₁₆Ge₃₀ the Hall resistivity is relatively constant for temperatures from 150 to 300 K with values of 2×10^{-6} and -2.5×10^{-6} Ω cm, respectively. Assume a single carrier band yields a carrier concentration of 2.2×10^{21} holes cm^{-3} for

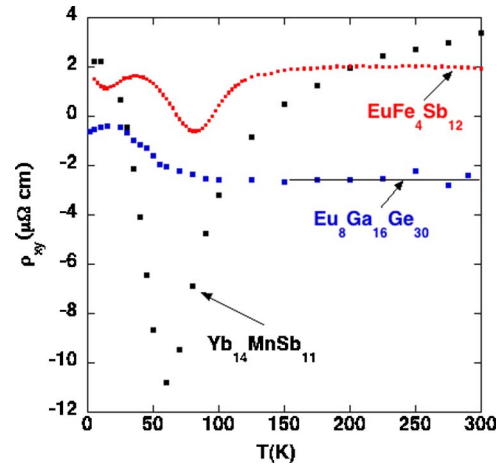


FIG. 5. (Color online) Hall resistivity vs temperature data for the three ferromagnets taken in a field of 7 T. For EuFe₄Sb₁₂ and Eu₈Ga₁₆Ge₃₀ the Hall resistivity is relatively constant for temperatures from 150 to 300 K with values of 2×10^{-6} Ω cm and -2.5×10^{-6} Ω cm, respectively. Assume a single carrier band yields a carrier concentration of 2.2×10^{21} holes cm^{-3} for EuFe₄Sb₁₂ and 1.75×10^{21} electrons cm^{-3} for Eu₈Ga₁₆Ge₃₀. The feature near 40 K in the Hall data from EuFe₄Sb₁₂ is related to a subtle change in the crystal structure. The Hall resistivity of Yb₁₄MnSb₁₁ well above $T_c \approx 53$ K has a significant contribution from the AHE (with an applied field) even at room temperature. Analyses of these data using several models (see text) give a consistent value of 0.93×10^{21} holes cm^{-3} for $100\text{ K} < T < 300\text{ K}$.

EuFe₄Sb₁₂ and 1.75×10^{21} electrons cm^{-3} for Eu₈Ga₁₆Ge₃₀. The decrease in the Hall resistivity of EuFe₄Sb₁₂ below 40 K is related to a large anomaly in the elastic constants,³⁰ which may reflect a subtle change in the crystal structure. Only the Hall resistivity of Yb₁₄MnSb₁₁ well above $T_c \approx 53$ K has a significant contribution from the AHE even at room temperature. This anomalous contribution to the Hall resistivity above T_c (in an applied field of 7 T) is large and measurable because at high temperatures the resistivity of Yb₁₄MnSb₁₁ is about 3–5 times larger than the other two compounds, but also because Kondo physics appears to be important in Yb₁₄MnSb₁₁.^{15,24} As discussed in Ref. 15, the Hall data of Yb₁₄MnSb₁₁ from 100 to 300 K can be accurately described by a constant plus a Curie-Weiss term or a constant plus a Curie-Weiss term times the resistivity (or resistivity squared). All three fits to the data give very similar values for the constant, which corresponds to a carrier concentration for this crystal of 9.3×10^{20} holes cm^{-3} . At 5 K the magnetization for each compound is nearly constant for fields greater than 2 T, and the linear slope of the Hall resistivity for $H > 2$ T can be used to estimate the carrier concentration (assuming one carrier band). At 5 K the carrier concentrations are found to be 3.5×10^{21} holes cm^{-3} , 1.55×10^{21} electrons cm^{-3} , and 1.1×10^{21} holes cm^{-3} , for EuFe₄Sb₁₂, Eu₈Ga₁₆Ge₃₀, and Yb₁₄MnSb₁₁, respectively. These values are not too far from those estimated from the data well above T_c . The carrier concentration of 1.55×10^{21} electrons cm^{-3} found for the Eu₈Ga₁₆Ge₃₀ single crystal at 5 K is similar to the value of 1.25×10^{21} electrons cm^{-3} previously found by Paschen *et al.*²¹ for a polycrystalline sample at 2 K.

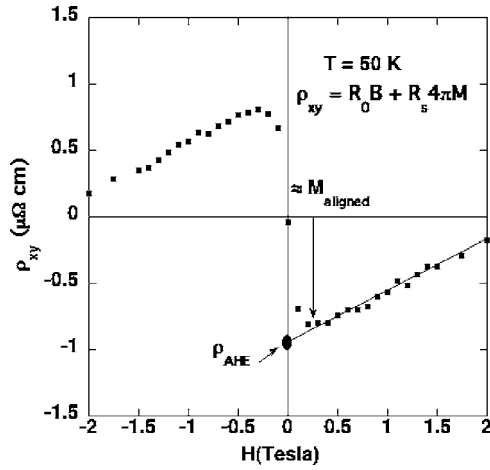


FIG. 6. Example of how the zero field contribution to the anomalous Hall resistivity, $\rho_{\text{AHE}} = \rho'_{\text{xy}}$ is determined. The data shown is the measured Hall resistivity of $\text{EuFe}_4\text{Sb}_{12}$ at 50 K as a function of applied field.

The anomalous Hall resistivity in the limit of zero applied magnetic field is determined from isothermal plots of the Hall resistivity versus applied magnetic field for $T < T_c$. An example of the analysis used is shown in Fig. 6. The Hall resistivity data for fields larger than the value needed to align the domains (denoted as M_{aligned} in the figure) are extrapolated back to $H=0$. This intercept is the anomalous portion of the Hall resistivity $\rho_{\text{AHE}} = \rho'_{\text{xy}}$. For each compound, ρ'_{xy} is determined in this manner at several temperatures below T_c . The isothermal plots of the Hall resistivity versus field for the three ferromagnets are shown in Figs. 7–9.

ANALYSIS AND DISCUSSION

As discussed in the Introduction, theory suggests that ρ'_{xy} can be described by an extrinsic contribution that is proportional to ρ and an intrinsic contribution proportional to ρ^2 so that $\rho'_{\text{xy}} = \sigma'_{\text{xy}}\rho^2 + a\rho$, and to be consistent with recent theoretical calculations $\sigma'_{\text{xy}} = \sigma_{\text{xy}}$. At low temperatures, $T < 0.2 T_c$,

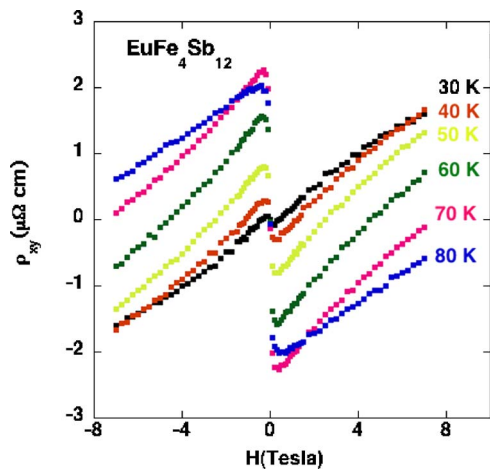


FIG. 7. (Color online) Isothermal Hall resistivity vs magnetic field data from a polycrystalline sample of $\text{EuFe}_4\text{Sb}_{12}$.

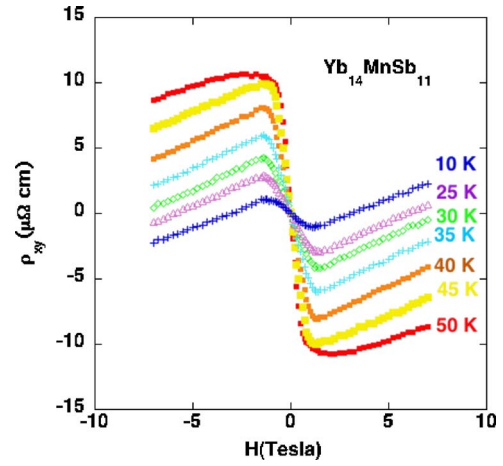


FIG. 8. (Color online) Isothermal Hall resistivity vs magnetic field data from a single crystal of $\text{Yb}_{14}\text{MnSb}_{11}$ with $H \parallel (110)$ and the current along the c axis.

where the spontaneous magnetization is nearly constant, linear fits to plots of ρ'_{xy}/ρ versus ρ can be used to determine σ_{xy} and a . However, this does not use most of the experimental data that is taken between 0.2 and $\approx 0.9 T_c$. If we assume that σ_{xy} and a have no intrinsic variation with temperature except through the variation of the magnetization order parameter with temperature, then $\rho'_{\text{xy}} = [M(T)/M(0)] [\sigma_{\text{xy}}^0 \rho^2 + a^0 \rho]$, where σ_{xy}^0 and a^0 are the values of σ_{xy} and a at $T=0$. Calculations⁸ of σ_{xy} for Fe as a function of temperature indicate that from $T=0$ to $T=300$ K, σ_{xy} does not change much with temperature although even at 300 K, $T < 0.3 T_c$ of Fe. We make the further assumption that σ_{xy} and a are proportional to the spontaneous magnetization as T approaches T_c . This assumption is motivated by the original empirical observation by Hall that ρ'_{xy} is proportional to M and, as shown below, this approximation seems to hold for the three ferromagnetic compounds investigated in this article. It also appears to be valid in the recent investigation³¹ of the AHE in ferromagnetic thin films of Mn_5Ge_3 . However, it is important to note that in some ferromagnetic compounds with un-

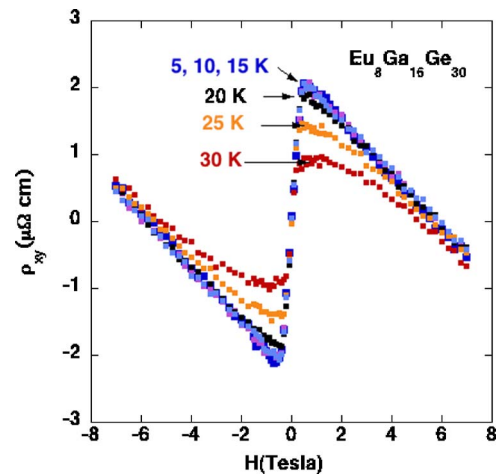


FIG. 9. (Color online) Isothermal Hall resistivity vs magnetic field data from an unoriented crystal of $\text{Eu}_8\text{Ga}_{16}\text{Ge}_{30}$.

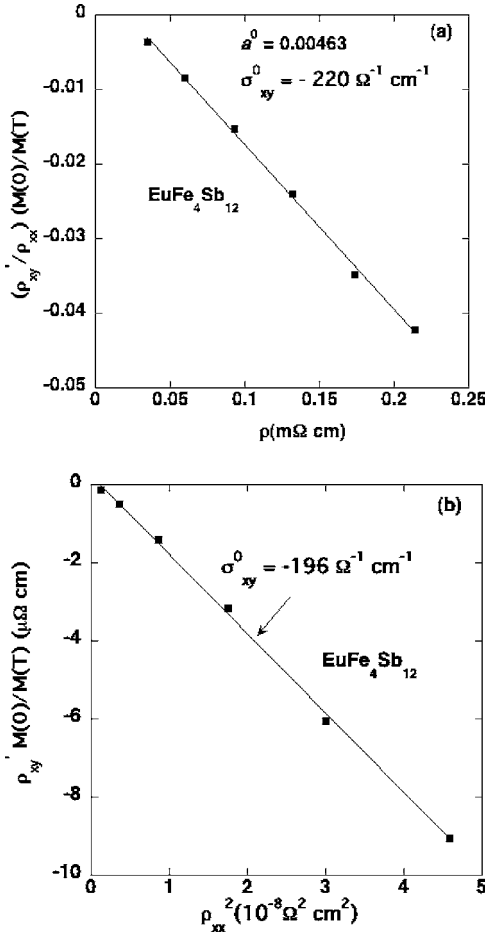


FIG. 10. (a) Analysis of the intrinsic and extrinsic contributions to the AHE of $\text{EuFe}_4\text{Sb}_{12}$ from $\rho'_{xy} = [M(T)/M(0)] [\sigma_{xy}^0 \rho^2 + a^0 \rho]$. (b) Analysis of the intrinsic contribution to the AHE of $\text{EuFe}_4\text{Sb}_{12}$ assuming that skew scattering can be neglected ($\rho'_{xy} \approx [M(T)/M(0)] \sigma_{xy}^0 \rho^2$).

usual electronic structures, such as SrRuO_3 , the anomalous Hall effect is not a simple linear function of the spontaneous magnetization.^{32–34}

Plots of $M(0)/M(T) [\rho'_{xy}/\rho]$ vs ρ are shown in Fig. 10(a) for $\text{EuFe}_4\text{Sb}_{12}$. The variation of the magnetization and resistivity with temperature is taken from the data shown in Figs. 3–5. The data are well described by a line with $\sigma_{xy}^0 = -220 \Omega^{-1} \text{cm}^{-1}$ and $a^0 = 0.0046$. If we assume that the extrinsic contribution to ρ'_{xy} from a stoichiometric compound can be neglected, i.e., $M(0)/M(T) (\rho'_{xy}) \approx \sigma_{xy}^0 \rho^2$, then analysis of the $\text{EuFe}_4\text{Sb}_{12}$ data neglecting skew scattering [Fig. 10(b)] gives $\sigma_{xy}^0 = -196 \Omega^{-1} \text{cm}^{-1}$. Although $\text{EuFe}_4\text{Sb}_{12}$ exhibits the largest relative decrease in resistivity below T_c , the magnitude of ρ'_{xy} below 25 K is below our detectability limit for a bulk sample (see Fig. 7). The resistivity of $\text{EuFe}_4\text{Sb}_{12}$ at $T = 2$ K is about $7.5 \mu\Omega \text{cm}$ which is too metallic to directly measure the expected value of ρ'_{xy} of $3.5 \times 10^{-8} \Omega \text{cm}$. A similar analysis of the $\text{Yb}_{14}\text{MnSb}_{11}$ data shown in Fig. 8 results in values of $a^0 = -0.0033$ and $\sigma_{xy}^0 = -14.7 \Omega^{-1} \text{cm}^{-1}$ [Fig. 11(a)] or $\sigma_{xy}^0 = -19 \Omega^{-1} \text{cm}^{-1}$ if skew scattering is neglected [Fig. 11(b)]. As can be seen from Fig. 8, at the lowest temperature (10 K for this figure) the intercept ρ'_{xy} can

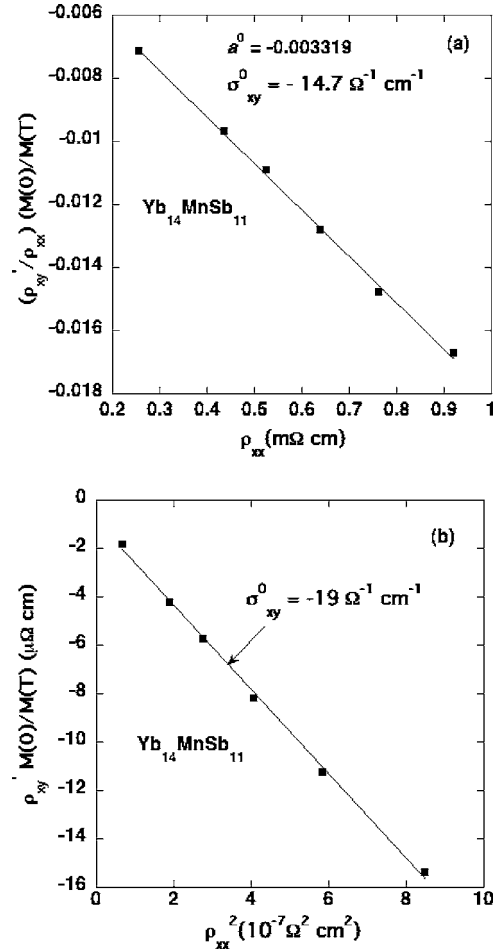


FIG. 11. (a) Analysis of the intrinsic and extrinsic contributions to the AHE of $\text{Yb}_{14}\text{MnSb}_{11}$ assuming $\rho'_{xy} = [M(T)/M(0)] [\sigma_{xy}^0 \rho^2 + a^0 \rho]$. (b) Analysis of the intrinsic contribution to the AHE of $\text{Yb}_{14}\text{MnSb}_{11}$ assuming that skew scattering can be neglected ($\rho'_{xy} \approx [M(T)/M(0)] \sigma_{xy}^0 \rho^2$).

be clearly extracted from the data. This is also true for all temperatures below 10 K down to our lowest attainable temperature of 2 K (data not shown in Fig. 8). The ability to measure ρ'_{xy} for the $\text{Yb}_{14}\text{MnSb}_{11}$ crystal down to the lowest temperatures is related to the large residual resistivity ($\approx 200 \mu\Omega \text{cm}$). The resistivity of $\text{Eu}_8\text{Ga}_{16}\text{Ge}_{30}$ only varies by about 30% below $T_c = 36$ K. This implies that there is not much variation ρ'_{xy} which makes it impossible to accurately decompose ρ'_{xy} into intrinsic and extrinsic components. As can be seen from Fig. 9, the extrapolated intercept of the Hall resistivity data to $H = 0$ (ρ'_{xy}) does not vary much from 5 to 20 K, and there is not much variation at 25 or 30 K once the change in magnetization is accounted for. For these data we were unable to determine both σ_{xy}^0 and a^0 , because the value and sign of a depended on exactly how the extrapolation from higher fields was done. There is not enough information in the data (Fig. 9) to determine both σ_{xy} and a . The best we can do is to give an average value for σ_{xy} . Analysis of the data in Fig. 9 assuming $M(0)/M(T) (\rho'_{xy}) \approx \sigma_{xy}^0 \rho^2$, gives $\sigma_{xy}^0 \approx 28 \pm 3 \Omega^{-1} \text{cm}^{-1}$ (Fig. 12). An approximate analysis of the Hall data previously reported by Pas-

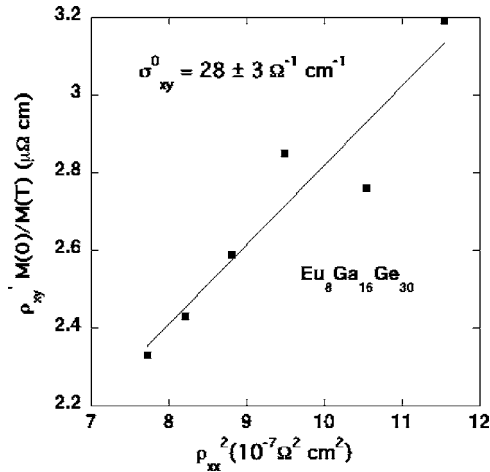


FIG. 12. Approximate analysis of the total anomalous Hall resistivity vs temperature of $\text{Eu}_8\text{Ga}_{16}\text{Ge}_{30}$ assuming $\rho'_{xy} \approx [M(T)/M(0)]\sigma_{xy}^0\rho^2$. The small variation of the resistivity of $\text{Eu}_8\text{Ga}_{16}\text{Ge}_{30}$ below T_c makes it impossible to accurately separate the Hall resistivity into intrinsic and extrinsic components.

chen *et al.*²¹ on a polycrystalline sample of $\text{Eu}_8\text{Ga}_{16}\text{Ge}_{30}$ yields $\sigma_{xy}^0 \approx 22 \Omega^{-1} \text{ cm}^{-1}$.

We were curious as to how the fraction of the intrinsic contribution to the AHE varied with temperature. The values of a^0 and σ_{xy}^0 determined for $\text{EuFe}_4\text{Sb}_{12}$ and $\text{Yb}_{14}\text{MnSb}_{11}$ are used to estimate the fraction of ρ'_{xy} that is intrinsic as the temperature is varied from $T=0$ to about $0.9 T_c$ (Fig. 13). At the lowest temperatures more than half of ρ'_{xy} is due to an extrinsic contribution linear in ρ such as skew scattering. This is rather surprising since ρ'_{xy} can also be described fairly well by a single term proportional to ρ^2 [Figs. 10(b) and 11(b)]. This means that fairly linear plots of ρ'_{xy} vs ρ^2 do not necessarily imply that there is no extrinsic contribution. Plots of ρ'_{xy}/ρ vs ρ are clearly a more sensitive way to separate intrinsic and extrinsic components.

Some relevant properties from all three ferromagnets are summarized in Table I. There are several important observations. There is clearly a substantial and finite intrinsic con-

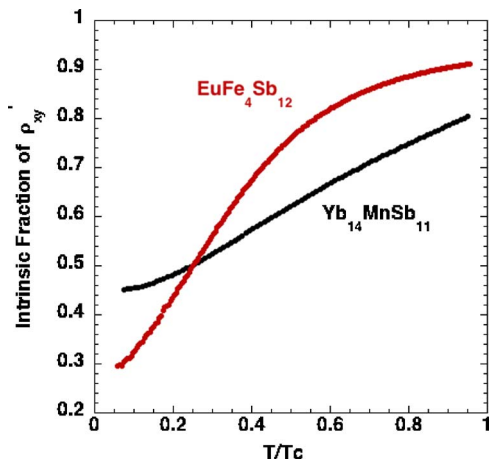


FIG. 13. (Color online) Variation of the intrinsic fraction of the AHE with temperature as determined from the fits to the data in Figs. 10(a) and 11(a), and using the resistivity data in Fig. 4.

TABLE I. Selected properties of the three ferromagnets.

Compound	$\text{EuFe}_4\text{Sb}_{12}$	$\text{Yb}_{14}\text{MnSb}_{11}$	$\text{Eu}_8\text{Ga}_{16}\text{Ge}_{30}$
T_c (K)	84	53	36
$4\pi M_o$ (Gauss)	1560	615	5535
$n_{\text{high } T}$ (10^{21} cm^{-3})	2.2	0.93	-1.75
$n_{5 \text{ K}}$ (10^{21} cm^{-3})	3.54	1.1	-1.55
a^0	0.0046	-0.0033	...
σ_{xy}^0 ($\Omega^{-1} \text{ cm}^{-1}$)	-220	-14.7	28 ± 3

tribution to ρ'_{xy} as T approaches 0. This result supports recent theories,^{8,35,36} which attribute the intrinsic AHE to a ground state property that can be determined from electronic structure calculations. The excellent linear variation of $M(0)/M(T)$ [ρ'_{xy}/ρ] vs ρ over a wide range of temperatures and resistivities implies that both a and σ_{xy} can only weakly depend on temperature. A weak variation of σ_{xy} with temperature was theoretically predicted for iron at temperatures below 300 K. The present results suggest that for these compounds this weak variation may hold for all temperatures below T_c if the temperature variation of the spontaneous magnetization is taken into account. For all three ferromagnets, the sign of σ_{xy} is opposite to the normal Hall component. This was also the case in a careful recent study on Co films⁷ but in older studies³⁷ on Gd crystals, and on various transition metal films³⁸ σ_{xy} appears to have the same sign as the normal Hall component. Current theory^{8,31,35,36} has shown that the sign of the intrinsic Hall conductivity is dominated by specific “hot spots” in the electronic structure and has no simple relationship to the sign of the normal Hall coefficient. The magnitude of $\sigma_{xy}^0 = 220 \Omega^{-1} \text{ cm}^{-1}$ for $\text{EuFe}_4\text{Sb}_{12}$ is much larger than the values of $\sigma_{xy}^0 \approx 10\text{--}30 \Omega^{-1} \text{ cm}^{-1}$ found for the other two ferromagnets. The value for $\text{EuFe}_4\text{Sb}_{12}$ is similar to the value of $240 \Omega^{-1} \text{ cm}^{-1}$ found for Co films and is probably related to the weak itinerant magnetism associated with the Fe $3d$ bands. It would be interesting if theory could calculate σ_{xy} for $\text{EuFe}_4\text{Sb}_{12}$ or the related weak ferromagnet $\text{NaFe}_4\text{Sb}_{12}$.²⁷ While the values of σ_{xy} for $\text{Yb}_{14}\text{MnSb}_{11}$ and $\text{Eu}_8\text{Ga}_{16}\text{Ge}_{30}$ are substantially smaller than found for $\text{EuFe}_4\text{Sb}_{12}$, they are comparable to the “gigantic anomalous Hall effect” found³⁹ in the magnetically complex pyrochlore $\text{Nd}_2\text{Mo}_2\text{O}_7$. Another observation is that the magnitude of the extrinsic skew scattering coefficient, a^0 , is about the same for the two crystals where it could be accurately determined ($|a^0| \approx 0.004$). This may indicate a similar degree of disorder and defects in the two materials.^{7,31} Finally, the recent ideas of the AHE have only been carefully tested on relatively simple materials such as Fe⁸ and Co⁷ and a few other ferromagnets.^{31–34,39} The apparent applicability of these ideas to considerably more complex ferromagnets, bodes well for our general understanding of the origin of the AHE.

ACKNOWLEDGMENTS

It is a pleasure to acknowledge stimulating and illuminat-

ing discussions with Allan MacDonald, David Singh, Thomas Schulthess, V. V. “Krishna” Krishnamurthy, Veerle Keppens, Sriparna Bhattacharya, and Raphael Hermann. Research was sponsored by the Division of Materials Sciences

and Engineering, Office of Basic Energy Sciences, U.S. Department of Energy, under Contract No. DE-AC05-00OR22725 with Oak Ridge National Laboratory, managed and operated by UT-Battelle, LLC.

-
- ¹E. H. Hall, *Philos. Mag.* **10**, 301 (1880).
²E. H. Hall, *Philos. Mag.* **12**, 157 (1881).
³J. Smit, *Physica (Amsterdam)* **21**, 877 (1955).
⁴J. Smit, *Physica (Amsterdam)* **24**, 39 (1958).
⁵L. Berger, *Phys. Rev. B* **2**, 4559 (1970).
⁶R. Karpplus and J. M. Luttinger, *Phys. Rev.* **95**, 1154 (1954).
⁷J. Kotzler and W. Gil, *Phys. Rev. B* **72**, 060412(R) (2005).
⁸Y. Yao, L. Kleinman, A. H. MacDonald, J. Sinova, T. Jungwirth, D.-S. Wang, E. Wang, and Q. Niu, *Phys. Rev. Lett.* **92**, 037204 (2004).
⁹P. N. Dheer, *Phys. Rev.* **156**, 637 (1967).
¹⁰W. Lee, S. Watauchi, V. L. Miller, R. J. Cava, and N. P. Ong, *Science* **303**, 1647 (2004).
¹¹J. D. Corbett, *Chem. Rev. (Washington, D.C.)* **85**, 383 (1985).
¹²B. C. Sales, in *Handbook of Phys. and Chem. Rare Earths: Filled Skutterudites*, edited by K. A. Gschneidner (Elsevier, New York, 2003), Vol. 33, Chap. 211, p. 1.
¹³B. C. Sales, B. C. Chakoumakos, and D. Mandrus, *Phys. Rev. B* **61**, 2475 (2000).
¹⁴I. R. Fisher, T. A. Wiener, S. L. Budko, P. C. Canfield, J. Y. Chan, and S. M. Kauzlarich, *Phys. Rev. B* **59**, 13829 (1999).
¹⁵B. C. Sales, P. Khalifah, T. P. Enck, E. J. Nagler, R. E. Sykora, R. Jin, and D. Mandrus, *Phys. Rev. B* **72**, 205207 (2005).
¹⁶B. C. Sales, B. C. Chakoumakos, R. Jin, J. R. Thompson, and D. Mandrus, *Phys. Rev. B* **63**, 245113 (2001).
¹⁷E. D. Bauer, A. Slebarski, N. A. Frederick, W. M. Yuhasz, M. B. Maple, D. Cao, F. Bridges, G. Geister, and P. Rogl, *J. Phys.: Condens. Matter* **16**, 5095 (2004).
¹⁸E. Bauer, St. Berger, A. Galatanu, M. Galli, H. Michor, G. Hilscher, Ch. Paul, B. Ni, M. M. Abd-Elmeguid, V. H. Tran, A. Grytsiv, and P. Rogl, *Phys. Rev. B* **63**, 224414 (2001).
¹⁹J. Y. Chan, M. M. Olmstead, S. M. Kauzlarich, and D. J. Webb, *Chem. Mater.* **10**, 3583 (1998).
²⁰P. Fazekas, *Lecture Notes on Electron Correlation and Magnetism* (World Scientific, Singapore, 1999), p. 643.
²¹S. Paschen, W. Carrillo-Cabrera, A. Bentien, V. H. Tran, M. Baenitz, Yu. Grin, and F. Steglich, *Phys. Rev. B* **64**, 214404 (2001).
²²R. Hermann (private communication).
²³I. Zerec, V. Keppens, M. A. McGuire, D. Mandrus, B. C. Sales, and P. Thalmeier, *Phys. Rev. Lett.* **92**, 185502 (2004).
²⁴K. S. Burch, A. Schafgans, N. P. Butch, T. A. Sayles, M. B. Maple, B. C. Sales, D. Mandrus, and D. N. Basov, *Phys. Rev. Lett.* **95**, 046401 (2005).
²⁵T. C. Schulthess, W. M. Temmerman, Z. Szotek, W. H. Butler, and G. M. Stocks, *Nat. Mater.* **4**, 838 (2005).
²⁶W. Schnelle, A. Leithe-Jasper, M. Schmidt, H. Rosner, H. Borrmann, U. Burkhardt, J. A. Mydosh, and Y. Grin, *Phys. Rev. B* **72**, 020402(R) (2005).
²⁷A. Leithe-Jasper, W. Schnelle, H. Rosner, M. Baenitz, A. Rabis, A. A. Gippius, E. N. Morozova, H. Borrmann, U. Burkhardt, R. Ramlau, U. Schwarz, J. A. Mydosh, Y. Grin, V. Ksenofontov, and S. Reiman, *Phys. Rev. B* **70**, 214418 (2004).
²⁸A. Leithe-Jasper, W. Schnelle, H. Rosner, N. Senthilkumaran, A. Rabis, M. Baenitz, A. Gippius, E. Morozova, J. A. Mydosh, and Y. Grin, *Phys. Rev. Lett.* **91**, 037208 (2003).
²⁹V. V. Krishnamurthy (private communication).
³⁰Sriparna Bhattacharya (private communication).
³¹C. Zeng, Y. Yao, Q. Niu, and H. H. Weitering, *Phys. Rev. Lett.* **96**, 037204 (2006).
³²Z. Fang, N. Nagosa, K. S. Takahashi, A. Asamitsu, R. Mathieu, T. Ogasawara, H. Yamada, M. Kawasaki, Y. Tokura, and K. Terakura, *Science* **302**, 92 (2003).
³³R. Mathieu, A. Asamitsu, H. Yamada, K. S. Takahashi, M. Kawasaki, Z. Fang, N. Nagosa, and Y. Tokura, *Phys. Rev. Lett.* **93**, 016602 (2004).
³⁴M. Onoda and N. Nagosa, *J. Phys. Soc. Jpn.* **71**, 19 (2002).
³⁵T. Jungwirth, Q. Niu, and A. H. MacDonald, *Phys. Rev. Lett.* **88**, 207208 (2002).
³⁶I. V. Solovyev, *Phys. Rev. B* **67**, 174406 (2003).
³⁷R. S. Lee and S. Legvold, *Phys. Rev.* **162**, 431 (1967).
³⁸S. P. McAlister and C. M. Hurd, *J. Appl. Phys.* **50**, 7526 (1979).
³⁹Y. Taguchi, Y. Oohara, H. Yoshizawa, N. Nagaosa, and Y. Tokura, *Science* **291**, 2573 (2001).